Received: 14 October 2025 | Revised: 29 April 2026 | Accepted: 13 June 2026

DOI: 10.1002/suco.70698

ARTICLE

fib CEB-FIP WILEY

Concrete with a very high number of load cycles—Identification of stress levels for efficient investigation of fatigue behavior

Kerstin Willers | **Lutz Gerlach** | **Frank Dehn**

Karlsruhe Institute of Technology (KIT), Institute of Concrete Structures & Building Materials, Building Materials and Concrete Construction, Karlsruhe, Germany

Correspondence
Kerstin Willers, Karlsruhe Institute of Technology (KIT), Institute of Concrete Structures & Building Materials, Building Materials and Concrete Construction, 76131 Karlsruhe, Germany.
Email: kerstin.willers@kit.edu

Funding information
Deutsche Forschungsgemeinschaft, Grant/Award Number: 504102079

Abstract

Fatigue stresses are receiving increasing attention in structural engineering, particularly in the design of increasingly slender structures. However, the mechanical response of concrete—particularly its fatigue behavior under very high numbers of load cycles—is still scarcely understood. Conventional fatigue testing is extremely time-consuming, whereas increasing the loading frequency may lead to specimen overheating. Additionally, dynamic or inertia effects are to be considered concerning high frequency testing. This paper proposes a conceptual approach to determine cyclic stress levels causing fatigue failure in the very high cycle fatigue (VHCF). A test frequency of approximately 85 Hz, applied using a high-frequency pulsator with oscillating adapters, was found to be suitable for concrete cylindrical specimens with a diameter-to-height-ratio of 30 mm/90 mm. Potential dynamic effects of the test equipment were taken into account during result evaluation, thereby validating the proposed test method. Furthermore, the temperature increase of the specimens during testing was recorded, and its influence on the reduction of concrete compressive strength was considered. The study confirms that fatigue testing at approximately 85 Hz, when appropriately corrected for temperature effects as well as dynamic influences, provides reliable fatigue data comparable to those obtained from conventional low-frequency tests.

KEYWORDS

fatigue of concrete, high frequency pulsator, increased specimen temperature, surface temperature, VHCF

1 | INTRODUCTION

In addition to resistance to static loads, the durability of structural engineering structures also requires resistance to frequently recurring and cyclical loads which can cause fatigue-related failure.

Concrete is often used in prestressed systems. However, well-founded knowledge concerning the resistance of concrete subjected to a large number of load cycles is currently limited to the low cycle fatigue (LCF) up to $N = 10^5$ and the high cycle fatigue (HCF) up to $N = 10^7$. $N > 10^7$ load cycles are formally assigned to the very high

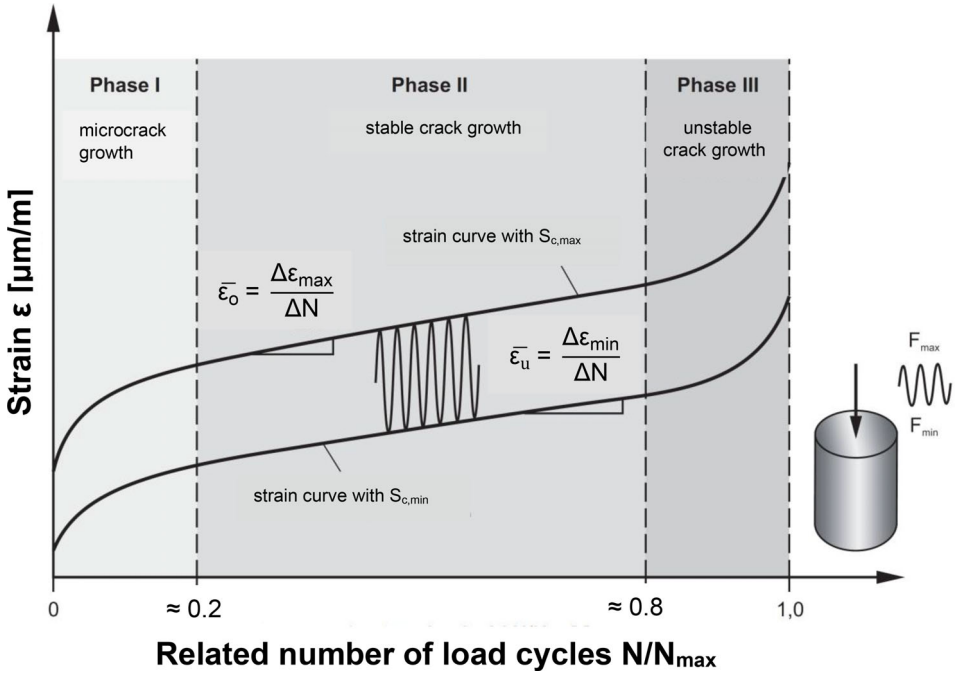

FIGURE 1 Compressive strain development under fatigue loading.[9]

cycle fatigue (VHCF).[1] Estimates of tolerable numbers of load cycles as a function of the stress level are usually presented in so-called S-N curves. S-N curves for concrete subjected to fatigue are included in the *fib* Model Code 2020[2] up to a number of load cycles of $N = 10^{20}$. The S-N curves were derived from fatigue tests with load cycles up to $N = 10^7$. However, the data on numbers of load cycles higher than $N = 10^7$ were determined exclusively by mathematical extrapolation.

Compared to a monotonously increasing compressive stress, fatigue stresses lead to an overall finer crack distribution and crack density[3] until fatigue failure, which especially for high-strength-concrete occurs suddenly.[4] Basic structural changes, specific damage phases and the change in stiffness under very high load cycles $N > 10^7$ have not yet been systematically investigated, analyzed and modeled in detail. Especially in the area of low stress ranges due to cyclic loads and high values of maximum stresses, results on fatigue tests are lacking, but this stress constellation is of extraordinary relevance for prestressed concrete structures.[5]

The fatigue strength of concrete under low-frequency loading depends on a large number of already known experimental boundary conditions such as the type of loading, the conditioning, the moisture content of the specimen, the loading rate or frequency, and the stress level.[3,6–8]

The compressive strain development as well as the change rate of stiffness with regard to minimum stress and maximum stress is characterized by three characteristic strain phases (see Figure 1) until failure.[7,8,10–13] The main reasons for the occurrence of the phase transitions

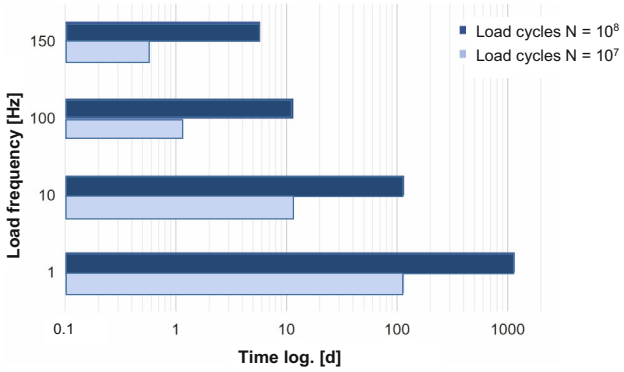

FIGURE 2 Necessary duration of fatigue tests in the VHCF range at different loading frequencies according to.[1]

as well as the duration of the degradation stages are almost unexplored for the range of very high numbers of load cycles. Due to the large number of material-specific and testing-related influences on the fatigue resistance of concrete, the topic of fatigue is a complex one.[12]

In order to be able to investigate the fatigue behavior of concrete in the range of very high numbers of load cycles within a time-feasible period, it is necessary to use high loading frequencies. Figure 2 illustrates the relevance of the change from high to very high load frequencies in order to be able to realize load cycles greater than $N = 10^7$.

However, high loading frequencies do not represent the real loading condition of cyclically loaded concrete structures, as these are mostly loaded with low loading frequencies <<1 Hz. Therefore, the influence of the loading frequency must be taken into account.

TABLE 1 Exemplary historical overview of fatigue research on concrete in the HCF.

Year of publication	References	Key research findings
1965	Murdock[16]	Failure in fatigue occurs in plain concrete members subjected to repeated or reversed flexural loads; no fatigue limit for the material is evident up to 10 million repetitions or reversals of load
1971	Awad and Hilsdorf[17]	A decrease in the maximum stress level, the stress range or the stress rate results in an increase in failure cycles; the static strength of concrete does not decrease continuously with the number of applied cycles
1973	Sparks and Menzies[6]	Linear relationship between the logarithm of the strain rate per cycle and the logarithm of the number of cycles to failure
1975	Weigler and Freitag[18]	There is no influence of test frequency within a range of $\sigma_o < 0{,}8 \cdot f_d$ concerning the number of load cycles
1978	Klausen[19]	Strain development under fatigue loading can be divided into three Phases
1979	Holmen[11]	The scatter in S-N-relationships concerning number of load cycles to failure at a given stress level can be explained form the scatter in static compressive strength; a reduction in the speed of testing seems to shorten the fatigue life especially at high stress levels
1992	Petkovic et al.[20]	No significant difference in behavior for fatigue in compression between high strength and lower strength concretes if the stresses are expressed relatively to the concrete strength
1992	Nygard et al.[21]	Environmental effect on fatigue is scale dependent
1993	Do et al.[22]	Strain development and stiffness degradation in relation to the number of load cycles in high-strength concrete were similar to those in normal-strength concrete; during Phase II a strong correlation was found between the logarithm of the strain rate and the logarithm of the number of cycles to failure, as well as between stiffness decrease rate and the number of cycles to failure
1996	Kim and Kim[23]	The fatigue life decreases with increasing the concrete strength; high strength concrete is more brittle than low strength concrete under fatigue loading
1998	Gao and Hsu[24]	The degradation of fatigue secant modulus can be used to describe the fatigue damage of concrete; irreversible strain caused by cyclic creep under action of average stress, caused by fatigue cracks and fatigue strain range
2004	Hohberg[10]	A frequency influence was observed in a range from approximately 0.1–10 Hz; higher or lower frequencies result in similar numbers of load cycles; water-stored specimens showed up to 10^3 times lower breaking load cycle counts than air-stored specimens
2005	Schwabach[25]	Structural damage resulting from cyclic loads is much more pronounced in areas of low stress intensity in normal concrete than in self-compacting concrete
2008	Ibuk[26]; Breitenbücher[27]	No significant or lasting "recovery-effect" during a test break were determined
2013	Saucedo et al.[28]	One-to-one correspondence between the logarithm of the secondary strain rate and the logarithm of the number of load cycles; with diminishing secondary strain rate, the fatigue life increases, secondary strain rate also depends on the stress ratio R and the frequency f
2015	Thiele[29]	Current damage condition cannot be determined based on the numbers of load cycles; the influence of specimen size is present in static and cycling loading conditions—larger specimens show lower numbers of load cycles
2016	von der Haar et al.[30]	Linear correlation between the logarithmic gradient of strain in Phase II and the logarithm of the number of load cycles despite different stress levels and test frequencies; surface heating of the specimens with increasing loading frequency
2018	Elsmeier[31,32]	The higher maximum compressive stress level and the higher frequency lead to a considerable increase in temperature; the increase in temperature could be caused by friction between the fine particles at the micro or nanoscale
2018	Hümme[33]	The average number of load cycles of the specimen tested under water were significantly below the S-N curves specified in the regulations

(Continues)

TABLE 1 (Continued)

Year of publication	References	Key research findings
2018	Schneider et al.[34]	For applied upper load stress of $S_o \leq 0.7$ the smaller test specimens exhibited significantly higher numbers of load cycles
2019; 2021	Tomann et al.,[35] Tomann[36]	The number of cycles to failure decreases with an increasing moisture content; the moisture content in the microstructure and not the wet environment is substantially responsible for the reduced fatigue resistance
2021	Deutscher et al.[37]	Fatigue tests with HPC and UHPC: Both concretes show a reduction in compressive strength with increasing concrete temperature

Tests in den VHCF within the scope of the joint research project WinConFat[14] were carried out on a total of three concretes of different strength classes. The results of the research project are summarized in.[15] Based on the unchangeable test parameters specified in the joint research project, only a few specimens of concrete strength class C120 showed failure in the fatigue tests. However, a specimen failure is essential in order to be able to describe all three damage Phases of concrete fatigue (see Figure 1). Therefore, the initial objective was to identify load levels that lead to fatigue failure in the VHCF range under a high loading frequency.

Concerning the time-constraint problem of fatigue testing with very high numbers of load cycles, a specific methodological solution to apply loads with high frequencies is necessary. The main goal is to identify stress levels that allow reliable testing in the VHCF within a reasonable time frame, a suitable specimen size, and without excessive specimen heating.

2 | CURRENT STATE OF RESEARCH ABOUT THE FATIGUE BEHAVIOR OF CONCRETE

The fatigue behavior of concrete in the HCF has been the focus of attention for several decades. An exemplary overview of fatigue tests on concrete from the last 60 years including the key research findings can be found in Table 1.

Summaries of the current state of research can also be found in reference 38.

Linear relationship between the increase in strain in Phase II and the number of load cycles was determined.[6,12,28,30]

Different findings have been reported with regard to test frequency. Saucedo et al.[28] also demonstrated a dependency on the stress ratio and loading frequency, which could not be identified in the aforementioned studies. While Weigler and Freitag[18] found no influence of test frequency on the number of load cycles within a range of $\sigma_o < 0.8 \cdot f_d$, Hohberg[10] noted that a frequency influence was observed only within a range from approximately 0.1 Hz to 10 Hz.

Elsmeier[31,32] point out that higher frequencies lead to a considerable increase in temperature. The increase in temperature could be caused by friction between fine particles at the micro or nanoscale.

With regard to specimen size larger specimens show lower numbers of load cycles.[29] However, in fatigue tests with an upper load stress of $S_o \leq 0.7$[34] smaller test specimens exhibited higher numbers of load cycles.

Load cycles of ≥10 million have only been considered in very few research studies. Table 2 provides a compilation of studies that have achieved load cycles in the VHCF.

The research results listed in Table 2 indicate that

- The specimen size varied across all research projects.
- Commonly used specimens with a diameter-to-height ratio of d/h=1.0/3.0 in HCF tests have not yet been investigated.
- Variations in test setups exist: The majority of the tests were carried out using hydraulic testing equipment (see references 18,19,39,40), whereas Karr et al.[41] and Fitzka et al.[42] applied loading using ultrasonic waves.
- In some cases, test pauses were implemented to allow specimen cooling (as the specimen temperature is not constant during fatigue testing).

The present study proposes a targeted approach to identifying purely mechanical fatigue failure in the VHCF without significant thermal failure and dynamic influences from the test setup. Therefore, small-scale test specimens with the diameter-to-maximum grain ratio of approximately 4.0 and a diameter-to-height ratio of d/h=1.0/3.0 are loaded at high frequency. Taking into account inertia effects of the test setup and increased specimen temperature during fatigue testing, the derived stress levels are determined through post-test evaluations. The results of a standardized, high-frequency, and time-efficient test method form the basis for identifying a stable high-frequency testing protocol that produces purely

TABLE 2 Compilation of testing and research on concrete behavior in the VHCF.

References	Specimen size [mm]	Strength of concrete f_{cm} or concrete type	$S_{c,min}$ [−]	$S_{c,max}$ [−]	Loading frequency [Hz]
Tepfers; Fridén und Georgsson[39]	Ø = 25 mm/h = 50 mm	20.9 N/mm²	0.14	0.70	150–200
			0.15	0.75	
			0.16	0.80	
			0.17	0.85	
Klausen[19]	Ø = 50 mm/h = 100 mm	44 N/mm²	0.05–0.4	0.63–0.84	200
Chen et al.[40]	Ø = 70 mm/h = 100 mm	C30	0.05–0.17	0.73–0,85	≤150
Weigler und Freitag[18]	Ø = 50 mm/h = 100 mm	Light weight concrete LB350/45 N/mm²	0.2–0.4	0.54–0.79	200
Karr et al.[41]	Ø ≈ 21 mm/h = 100 mm	80 N/mm²	0.06	0.44	750–1700 (discontinuous—200 ms with 20 kHz)
				0.50	
				0.56	
		107 N/mm²	0.04	0.38	
				0.43	
Willers et al.[9]	d/h = 30/60	129 N/mm² bzw. 139 N/mm²	0.2	0.65	ca. 130 Hz
			0.2	0.68	
			0.4	0.75	
			0.4	0.78	
			0.6	0.80	
Fitzka et al.[42]	Ø ≈ 21 mm/h = 35 mm	σ_{dB} = (133 ± 18) N/mm²	≈ 0.04	σ_{max} during a load cycle between 37% and 75% of the compressive strength σ_{dB}	19 kHz discontinuous (pulses of typically 4000 cycles are followed by pauses of 2–8 s) and 60 Hz servo-hydraulic loading

mechanical fatigue failures and allows a possible transfer to larger specimens tested at a low frequency.

3 | TEST EQUIPMENT, MEASUREMENT AND CONCRETE MIXTURE

3.1 | Technical implementation of the VHCF tests

For the VHCF tests, a high-frequency pulsator (HFP) ZwickRoell of the type 150HFP5000 was used. The basic prerequisite for carrying out compressive fatigue tests on concrete specimens was to provide the electromagnetically operated HFP with adapters generating an oscillating system for compression. By activating an electromagnet, the entire test system is excited at its natural frequency while compensating for any losses that occur.[43]

Compared to conventional fatigue tests, an oscillating system can affect the applied loads on the specimens due to inertia effects or control accuracy at high frequencies. These possible influences must be taken into account in order to be able to specify the upper and lower stress levels on the specimen.

3.2 | Verification of the oscillating system by an external load cell

To verify the oscillating test method concerning possible inertia effect, the deviation from the target values of the maximum and minimum load were determined with an external load cell used in addition to the specimen. For this purpose, selected stress levels were applied and the displayed forces of the external load cell were compared with those of the HFP and the target loads. Figure 3 shows a graphical comparison for a stress range of $S_{c,min} = 0.22$ and $S_{c,max} = 0.70$.

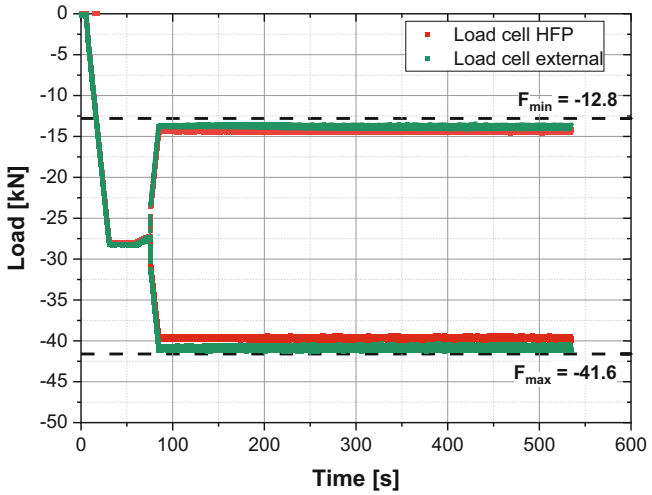

FIGURE 3 Comparison of the load curves of the external load cell, the load display of the HFP and the target loads for the selected load level.

TABLE 3 Concrete mixture.

Compressive strength class	C50/60
Consistency class	F5
CEM I 42,5 R	485 kg
0–2 Sand	726 kg
2–8 Gravel	890 kg
Water	195 kg
Superplasticiser	1% (in relation to the amount of cement)
w/c	0.40

The load values of the external load cell are used as basis in order to correctly apply the actual load in the subsequent analysis and evaluation of the concrete behavior. The resulting load levels can be found in Table 6, columns 4 and 5.

3.3 | Concrete mixture and specimens

A concrete of strength class C50/60 was used for the tests. The concrete composition is listed in Table 3.

All test specimens were produced within one concreting process with one concrete delivery batch. The specimens were stored for the first 28 days under moist jute fabrics at approximately 20°C. Afterwards, the specimens were stored in a climate chamber with constant conditions of 20°C and 65% relative humidity until the time of testing.

The specimen size, with a diameter-to-height ratio of d/h = 30 mm/90 mm, was chosen based on previous experience from the research project WinConFat,[14] as it has already been shown that a diameter of 30 mm does not lead to excessive specimen surface heating under high-frequency loading. The diameter is approximately four times the maximum aggregate size according to the requirements of DIN EN 12390-13:2021-09.[44] In this study, a loading frequency of approximately 85 Hz was applied.

TABLE 4 Concrete properties at 91 days.

Concrete cylinder: d/h = 30 mm/90 mm	
Compressive strength f_{cm} (22°C, 91 d)[a]	84.1 N/mm^2
Standard deviation	2.1 N/mm^2
Modulus of elasticity[b]	36,503 N/mm^2
Standard deviation	484 N/mm^2
Concrete cylinder: d/h = 150 mm/300 mm	
Compressive strength[c]	84.6 N/mm^2
Standard deviation	2.1 N/mm^2
Modulus of elasticity[b]	33,709 N/mm^2
Standard deviation	1128 N/mm^2

[a]Average value from the total of six results (one result was categorized as an outlier); ambient temperature of approximately 22°C.
[b]Average value from the total of three results.
[c]Average value from the total of six results.

The compressive strength at the age of 91 days, which was determined according to DIN EN 12390-3:2019-10[45] is given in Table 4. Additional compressive strength tests using concrete cylinders with the standard-compliant diameter-to-height ratio of d/h = 150 mm/300 mm in accordance with DIN EN 12390-1:2021-09[46] were carried out (see Table 4).

3.4 | Measurement equipment

An infrared sensor was used to record the surface temperature in the mid-height of the specimen. The ambient temperature was measured via a thermocouple in parallel. The strain development and the reduction of stiffness are characteristics which can be determined by two applied strain gauges opposite each other on the specimen in longitudinal direction. Figure 4 shows exemplary a concrete cylinder specimen used in the HFP.

4 | TEST RESULTS

The fatigue test results are summarized in Table 5, indicating the upper and lower stress levels and the estimated modulus of elasticity before cyclic loading according to DIN EN 12390-13:2021-09.[44]

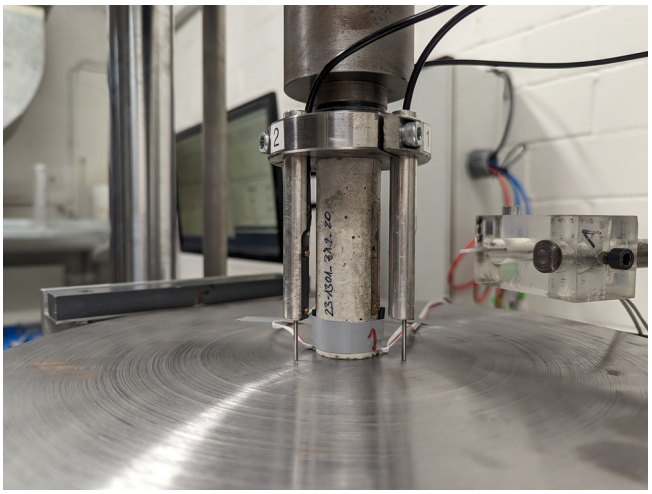

FIGURE 4 Specimen for fatigue tests in the HFP.

4.1 | Post-test evaluation of load stresses taking into account specimen heating as well as inertia effects in the test setup

The surface temperature in the fatigue tests occurring in Phase II $T_{P,II}$ (Phase II is determined between $N/N_{max} = 0.3$ to $N/N_{max} = 0.7$ here) ranges from approximately +32°C to +47°C (cf. Table 7). The heating of the concrete caused by cyclic tests leads to a reduction in the compressive strength of the concrete.[37] In order to estimate the reduction in concrete compressive strength the assumption, that the reduction of strength under monotonically increasing loads is comparable to the temperature effect in high-cycle tests, was made. Selected specimens were heated in a temperature chamber at approximately +35°C and approximately +45°C for ≥40 min. Then the concrete compressive strength was determined in an electromechanical testing machine Zwick 300 kN (see Figure 5).

The average concrete compressive strength at approximately +35°C and approximately +45°C is compared with the reference compressive strength determined at approximately +20°C. This results in a linear relationship (see Equation 1) shown in Figure 6. Due to the fact that post-hardening is considered to be mostly completed after 91 days, the different concrete ages of the specimens (91–281 days) are categorized as subordinate.

$$f_{cm}(T)/f_{cm}\left(22^{\circ}C, 91\,d\right) = -0.0068x + 1.1531 \qquad (1)$$

The stress levels specified in Table 6 show the initial stress levels (see columns 2 and 3), the changed stress levels taking into account a force measurement via an external load cell (see columns 4 and 5), and the derived stress levels taking into account the reduction of the concrete compressive strength according to Equation 1 as well (see columns 6 and 7).

In Table 8 strain-dependent results are mentioned such as the reduction of stiffness and the elastic strain components at the beginning of loading $\varepsilon_{el}{}^{0}$ and before failure $\varepsilon_{el}{}^{B}$.

4.2 | Effects of the post-test evaluation of load stresses

Taking into account heating of specimen and test-related influencing factors a shift of the initial stress levels to the derived stress levels occurs. These values were obtained as post-test evaluations. An increase of the initial upper

TABLE 5 Fatigue test on concrete cylinders with a loading frequency $f \approx 85$ Hz.

1	2	3	4
	Upper and lower stress level[a]		
	$S_{c,min}$	$S_{c,max}$	E-modulus[b]
Specimen designation	[−]	[−]	[N/mm²]
Z1.2_20	0.19	0.67	34,772
Z1.2_24	0.30	0.80	35,931
Z1.3_11	0.25	0.75	35,607
Z1.3_12	0.27	0.72	35,994
Z1.3_16	0.21	0.77	34,598
Z1.4_27	0.30	0.76	36,974
Z1.5_3	0.27	0.72	36,691
Z1.5_4_a + b	0.26	0.72	36,354

[a]Including temperature and load corrections (cf. derived stress levels in Table 6).
[b]Determined from the gradient prior loading between approximately 5% and 33% of the mean concrete compressive strength.

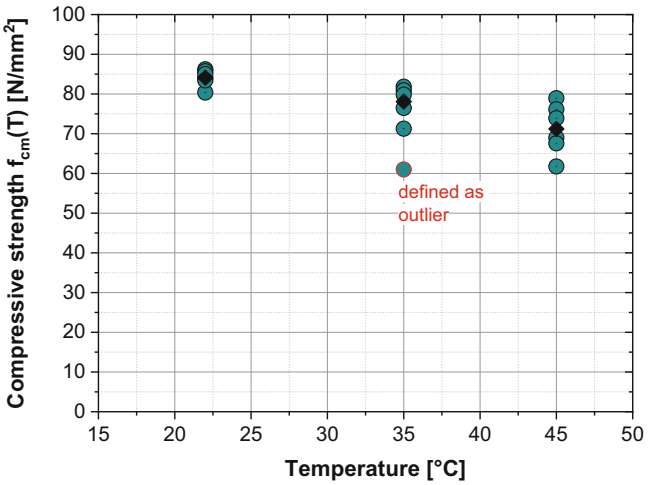

FIGURE 5 Test results of reduction in concrete compressive strength at approximately +35°C and approximately +45°C (temperature chamber storage) including average values.

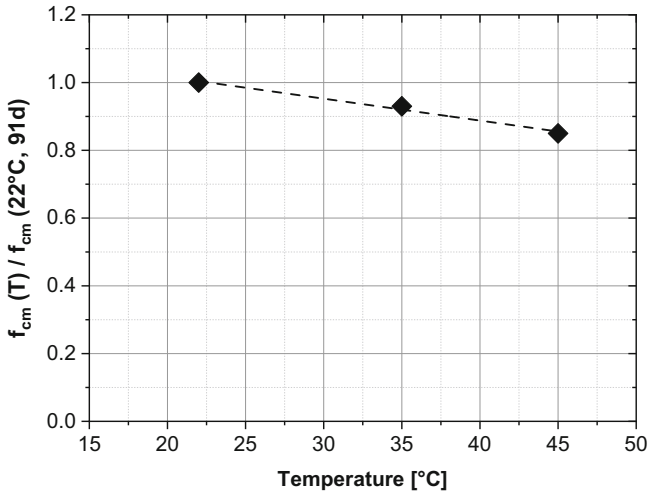

FIGURE 6 Regression function based on average values for estimating the percentage reduction in concrete compressive strength as a function of temperature.

and lower stress levels and, in most cases, a change in the initial stress range results. The shift ratios are listed in Table 9 in detail.

The greatest change in the initial stress level appears in the fatigue test with specimen no. Z1.3_16 with the lowest number of load cycles achieved. It can also be seen that an increase in the applied upper stresses, accompanied by a constant or increasing stress range, causes failure before the VHCF range (see specimens no. Z1.2_24, Z1.3_11, and Z1.3_16). The test results show that specimen heating and the effect of the test methodology are factors that must be taken into account to reflect the actual stress levels of the specimen within the fatigue tests.

The eight fatigue tests show number of load cycles which exceed the specifications in *fib* Model Code 2020[2] (see Figure 7). The S-N-curves in *fib* Model Code 2020[2] were developed based on experimental investigations which were carried out using cylindrical test specimens with a diameter-to-height ratio of d/h = 60 mm/180 mm.[47] Based on the small-scale specimens, the own test results have to be verified by larger specimens. It can be assumed that a size effect exists and larger specimens can withstand fewer number of load cycles at the same applied stress level.

4.3 | Development of strain at upper and lower stress level

The strain development at the upper and lower stress levels shows three phases I to III well known for the fatigue behavior of concrete in the HCF and LCF. The strain curves of specimen no. Z1.5_3 are shown as an example in Figure 8.

4.4 | Change in the fatigue secant moduli during the fatigue tests

In addition to the determination of the static modulus of elasticity, it is common practice in the field of concrete fatigue testing to determine the stiffness as the secant modulus during cyclic loading (e.g.,[11,25,48,49]). The fatigue secant modulus can be continuously recorded during the test using the strain values at upper and lower stress level and the associated stress in accordance with Equation 2. In addition to the secant modulus the static modulus of elasticity is shown graphically in Figure 9 also.

$$E_s = \frac{\sigma_{max} - \sigma_{min}}{\varepsilon_{max} - \varepsilon_{min}} \quad (2)$$

The material degradation or the development of damage under fatigue loading can be recorded on the basis of the continuous decrease in specimen stiffness and described by the changes in the secant modulus.[50] The secant modulus is therefore an indication of occurring structural damage.[51]

The fatigue tests carried out show a decrease in the fatigue secant modulus to between 82% and 95% of its initial value (see Table 8 and Figure 10). In particular, at the maximum stress range, the fatigue secant modulus decreases significantly more than in the other tests. For

TABLE 6 Determination of the stress levels taking into account an external force measurement and the reduction of the concrete compressive strength due to heating of the specimens.

1	2	3	4	5	6	7
Specimen designation	**Initial stress levels**		**Stress levels through the use of an external load cell**		**Derived stress levels (additional adjustment with use of an external load cell and regard to heating in Phase II)**[a]	
	$S_{c,min} = f_{c,min}/f_{cm(91d)}$	$S_{c,max} = f_{c,max}/f_{cm(91d)}$	$S_{c,min} = f_{c,min}/f_{cm(91d)}$	$S_{c,max} = f_{c,max}/f_{cm(91d)}$	$S_{c,min} = f_{c,min}/f_{cm(T)}$	$S_{c,max} = f_{c,max}/f_{cm(T)}$
	[−]	[−]	[−]	[−]	[−]	[−]
Z1.2_20	0.15	0.65	0.17	0.62	0.19	0.67
Z1.2_24	0.25	0.75	0.28	0.73	0.30	0.80
Z1.3_11	0.20	0.70	0.22	0.67	0.25	0.75
Z1.3_12	0.23	0.70	0.25	0.67	0.27	0.72
Z1.3_16	0.15	0.68	0.17	0.64	0.21	0.77
Z1.4_27	0.25	0.73	0.28	0.70	0.30	0.76
Z1.5_3	0.23	0.70	0.25	0.67	0.27	0.72
Z1.5_4_a + b	0.22	0.70	0.24	0.67	0.26	0.72

[a]These values were obtained as post-test evaluations.

the remaining stress ranges, the ratio E_S^B/E_S^0 changes only marginally within Phase II. Based on these results, an increase in the stress ranges appears to favor a reduction in the fatigue secant modulus more strongly than high upper stress levels.

Oneschkow[49] reported a reduction in stiffness to between 69% and 96% of the initial value for a high-strength concrete ($f_{c,cube,28d} = 116$ N/mm^2). Specimens with a diameter-to-height ratio of d/h = 60 mm/180 mm were tested at low-loading frequency.

The results of the present study fall within the range reported in,[49] but show a significantly smaller range of scatter. The current high-frequency tests appear to fail at a higher remaining stiffness on average, which could imply a significantly more brittle failure mechanism or a different damage accumulation process under high-frequency loading. Further investigations are necessary to clarify whether this assumption can be confirmed.

The elastic strain component prior to failure increases as the secant stiffness decreases. This relationship is well known in the HCF with low-frequency loading[51] and can also be confirmed for high-frequency tests. Specimen no. Z1.4_27 shows a slight decrease in secant stiffness accompanied by a slight elastic strain component prior to failure, whereas specimen no. Z1.2_20 shows a significant decrease in secant stiffness together with a significant increase in the elastic strain component prior to failure.

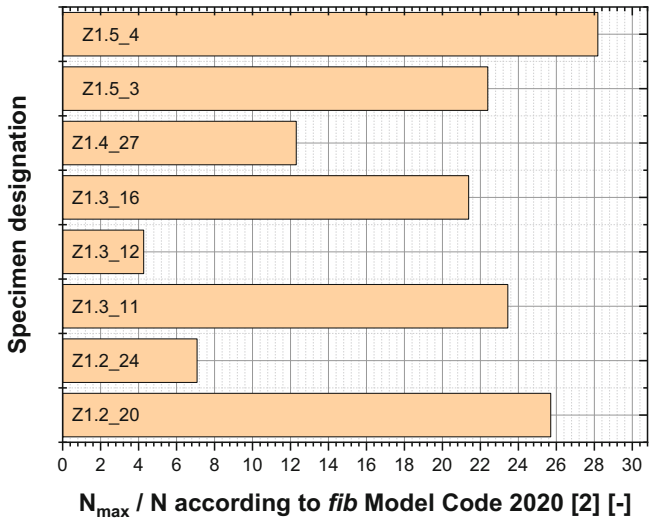

FIGURE 7 Ratio of number of load cycles from presented tests and number of load cycles according to *fib* Model Code 2020.[2]

4.5 | Temperature increase of the specimens at fatigue tests

An increase in surface temperature in fatigue-stressed concrete specimens has already been observed in several research studies in the HCF regime.[30–32,52] The heating, or the resulting thermal energy is related to the internal damping of the material[52,53] and is influenced by the loading frequency, stress amplitude, material properties and test duration. Larger stress amplitudes and higher

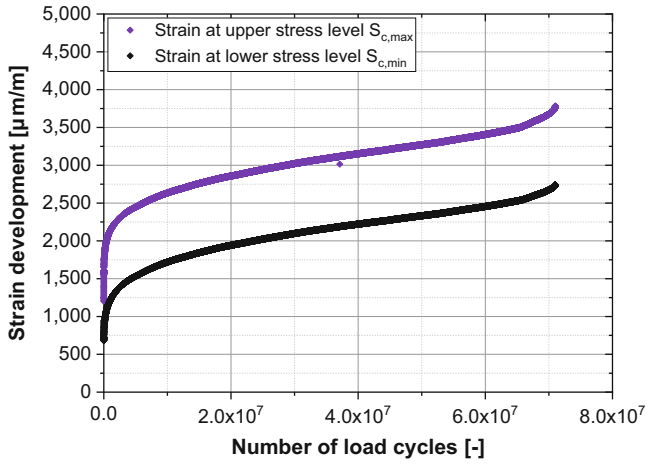

FIGURE 8 Strain curve of the fatigue test with specimen no. Z1.5.3.

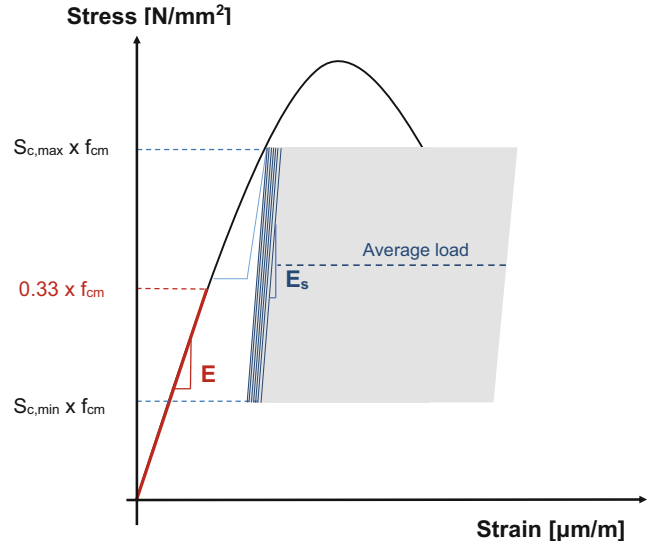

FIGURE 9 Modulus of elasticity and fatigue secant modulus.

loading frequencies lead to a higher heat release rate in the specimen and thus to faster heating.[54–56]

In addition to the ambient temperature (blue curve), the surface temperature measured at the mid-height of specimen no. Z1.2_20 (red curve) is shown as an example in Figure 11.

Figure 11 shows that the course of the specimen heating and the temperature difference are characterized by three phases.

The variation in ambient temperature is caused by on slight temperature differences due to the day-night cycle. The test results obtained from small specimens under high-frequency loading show a constant phase of surface temperature. This steady-state temperature condition occurs when internal heat generation reaches a constant value and a thermal equilibrium is established between

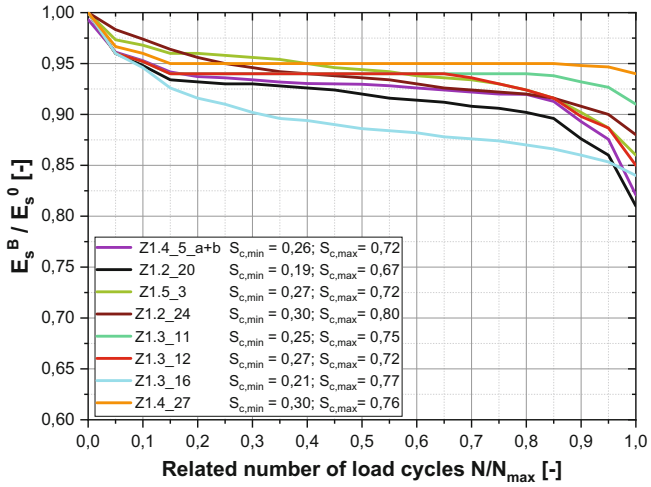

FIGURE 10 Reduction of the secant modules in the fatigue tests.

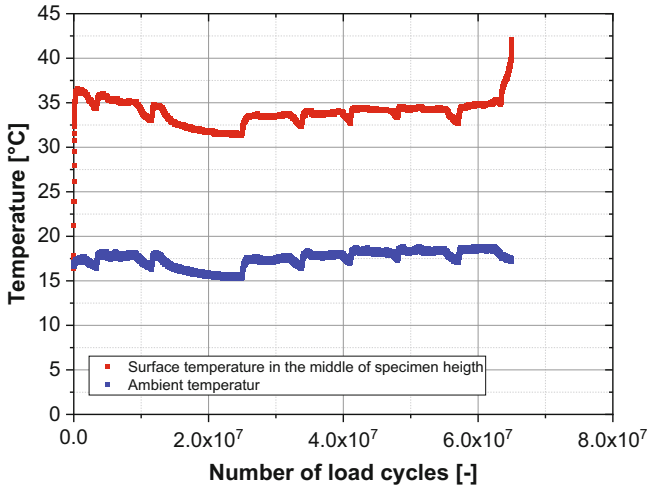

FIGURE 11 Surface temperature profile at the middle of the specimen height and ambient temperature during the fatigue test (no. Z1.2_20).

heat generation and heat dissipation through the outer surface of the specimen. There is no linear temperature increase with increasing temperature gradients, which could otherwise lead to premature specimen failure. This applies to all tested specimens—both those failing in the VHCF and those failing prior to it. This supports the validity of the testing method presented here.

4.6 | Logarithmic gradient of strain at upper stress level in Phase II

As part of the evaluation of the high-frequency tests, the increase in strain in Phase II at the upper and lower stress were determined (see Table 8).

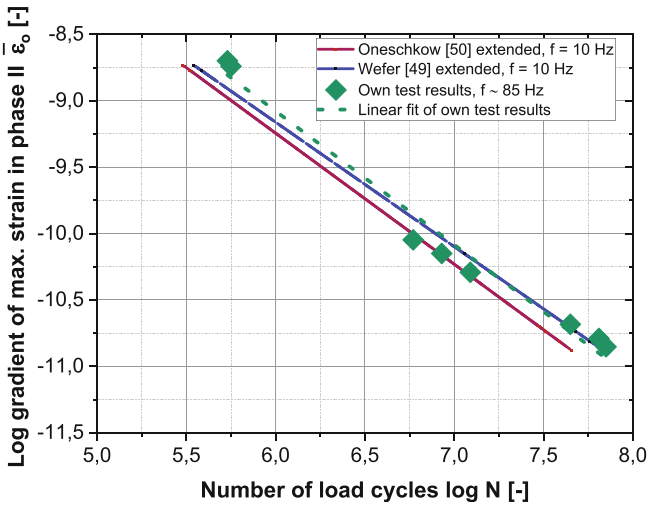

FIGURE 12 Comparison of logarithmic gradient of maximum strain in Phase II with the research results of Wefer[48] and Oneschkow.[49]

The present test results demonstrate a linear correlation between the logarithm of the number of load cycles and the logarithmic gradient in Phase II. Oneschkow[49] and Wefer[48] also reported linear dependencies between the logarithm of the number of load cycles and the logarithmic gradient of the maximum strain in Phase II.

When comparing results from all three research studies, a good agreement can be observed (see Figure 12) although different test frequencies are used. In contrast to the test results of Saucedo et al.,[28] no frequency dependence was detected. The research results indicate that only the increase in strain per load cycle in Phase II is of significant relevance.

5 | CONCLUSION AND OUTLOOK

To achieve sustainability goals in the construction sector, long service lives of concrete structures are required. With regard to cyclic loading, the fatigue behavior of concrete under load cycles exceeding 10 million has not yet been sufficiently investigated experimentally. In particular, the long duration of conventional fatigue tests conducted at low loading frequencies represents a major challenge.

This study investigates fatigue tests on concrete cylinders with a diameter-to-height ratio of 30 mm/90 mm using test frequencies of approximately 85 Hz in a HFP with oscillating adapters. Specimen heating as well as inertia effects induced by the test setup were explicitly considered. Consequently, the initially applied stress levels were converted into derived stress levels through post evaluations, which represent the actual stresses acting on the specimens. The derived stress levels indicate an increase in the lower stress level of 17%–40% and in the upper stress level of 3%–13% in relation to the initial stress levels.

The test results show that both the percentage reduction of the fatigue secant modulus E_S^B/E_S^0 during cyclic loading and the logarithmic strain gradient at the upper stress level in Phase II show a correlation with fatigue test results obtained in the high-cycle fatigue (HCF) range using larger specimens and significantly lower load frequencies. Despite the substantial difference in loading frequency, the test data in this study seems to be valid.

TABLE 7 Overview of the results of the fatigue tests.

1 Specimen designation	2 Max. strain at upper stress level	3 Max. strain at lower stress level	4 $T_{P,II}$	5 $\Delta T = T_{P,II} - T_R$	6 T_{final}	7 Log N_{max}[a]	8 Log N[a] according to *fib* Model Code 2020[2]
[−]	[μm/m]	[μm/m]	[°C]	[K]	[°C]	[−]	[−]
Z1.2_20	4082	2861	34.0	16.4	42.1	7.81	6.40
Z1.2_24	3256	2163	36.6	19.9	40.3	5.75	4.90
Z1.3_11	3171	2035	37.5	19.4	36.5	6.77	5.40
Z1.3_12	3354	2288	33.0	14.9	38.3	6.93	6.30
Z1.3_16	3125	1874	47.0	29.3	51.7	5.73	4.40
Z1.4_27	2959	2018	33.0	14.3	32.5	7.09	6.00
Z1.5_3	3781	2742	31.7	12.7	34.5	7.85	6.50
Z1.5_4_a + b	4419	3290	32.7	13.6	34.6	7.65	6.20

Note: $T_{P,II}$, surface temperature in the middle of the specimen height in Phase II. T_R, ambient temperature. T_{final}, surface temperature in the middle of the specimen height before failure.

[a]Base-10 logarithm is used.

TABLE 8 Strain-dependent results of the fatigue tests.

1 Specimen designation	2 Log. $\bar{\varepsilon}_o$	3 Log. $\bar{\varepsilon}_u$	4 E_S^0	5 E_S^B	6 E_S^B/E_S^0	7 ε_{el}^0	8 ε_{el}^B	9 $\varepsilon_{el}^B/\varepsilon_{el}^0$
[−]	[−]	[−]	[N/mm²]	[N/mm²]	[−]	[µm/m]	[µm/m]	[−]
Z1.2_20	−10.79	−10.81	39,796	34,031	0.86	1350	1668	1.24
Z1.2_24	−8.74	−8.77	41,325	36,235	0.88	1500	1718	1.15
Z1.3_11	−10.05	−10.03	41,441	34,957	0.84	1394	1656	1.19
Z1.3_12	−10.15	−10.15	41,524	35,659	0.86	1398	1629	1.16
Z1.3_16	−8.70	−8.73	39,482	33,162	0.84	1409	1679	1.19
Z1.4_27	−10.29	−10.30	42,033	40,091	0.95	1444	1500	1.04
Z1.5_3	−10.85	−10.88	42,959	36,441	0.85	1342	1597	1.19
Z1.5_4_a + b	−10.68	−10.70	41,724	34,128	0.82	1388	1701	1.23

Note: log. $\bar{\varepsilon}_o$, Logarithmic gradient of strain at upper stress level in Phase II (base-10 logarithm is used). log. $\bar{\varepsilon}_u$, Logarithmic gradient of strain at lower stress level in Phase II (base-10 logarithm is used). E_S^0, Fatigue secant modulus at the beginning of cyclic loading. E_S^B, Fatigue secant modulus at the ending of cyclic loading. ε_{el}^0, Elastic strain component at the beginning of cyclic loading[a]. ε_{el}^B, Elastic strain component at the ending of cyclic loading[a].
[a]The elastic strain component corresponds to the strain difference between the upper stress level and the relief. As approximation, the difference between the upper stress level and the intersection of the fatigue secant modulus with the X-axis is determined.

TABLE 9 Change of initial stress levels due to derived stress levels.

1 Specimen designation	2 Stress range (initial stress level)	3 Stress range (derived stress level)	4 $S_{c,min}$ (initial stress level)/ $S_{c,min}$ (derived stress level)	5 $S_{c,max}$ (initial stress level)/ $S_{c,max}$ (derived stress level)
	[−]	[−]	[−]	[−]
Z1.2_20	0.50	0.48	1.27	1.03
Z1.2_24	0.50	0.50	1.20	1.07
Z1.3_11	0.50	0.50	1.25	1.07
Z1.3_12	0.47	0.45	1.17	1.03
Z1.3_16	0.53	0.56	1.40	1.13
Z1.4_27	0.48	0.46	1.20	1.04
Z1.5_3	0.47	0.45	1.17	1.03
Z1.5_4_a + b	0.48	0.46	1.18	1.03

The following three initial stress level sets were identified as suitable for efficient VHCF testing:

- Stress level set I: $S_{c,min} \approx 0.15$; $S_{c,max} \approx 0.65$
- Stress level set II: $S_{c,min} \approx 0.22$; $S_{c,max} \approx 0.70$
- Stress level set III: $S_{c,min} \approx 0.25$; $S_{c,max} \approx 0.73$.

Specimens with a diameter-to-height-ratio of 30 mm/90 mm subjected to these fatigue loads reached numbers of load cycles >10 million (cf. Tables 6 and 7). Since no linear increase in temperature was observed, it can be assumed that a test frequency of approximately 85 Hz does not induce internal friction mechanisms leading to premature failure.

In future investigations, the three identified stress levels will be applied to additional small-scale specimens tested to high frequency to consolidate the results. In addition, fatigue tests on larger specimens with a diameter-to-height-ratio of 100 mm/300 mm at lower frequency will be conducted. This approach is necessary to assess potential size effects and to establish a link between high-frequency fatigue test results and the fatigue behavior of larger concrete specimens.

ACKNOWLEDGMENTS

This research was funded by the Deutsche Forschungsgemeinschaft (DFG, German Research Foundation). The investigations were carried out in the project

"Experimental tests on concrete in the range of very high numbers of load cycles as a basis for modelling the fatigue behaviour taking into account viscous and cyclic strain components" (project number: 504102079). Open Access funding enabled and organized by Projekt DEAL.

DATA AVAILABILITY STATEMENT

The data that support the findings of this study are available from the corresponding author upon reasonable request.

REFERENCES

1. Zimmermann M. Very High Cycle Fatigue. In: Schmauder S, Chen CS, Chawla K, Chawla N, Chen W, Kagawa Y, editors. Handbook of Mechanics of Materials. Singapore: Springer; 2018. https://doi.org/10.1007/978-981-10-6855-3_43-1
2. *fib* Model Code for Concrete Structures 2020. Fédération internationale du béton International Federation for Structural Concrete. Lausanne: International Federation of Structural Concrete; 2023.
3. König G, Danielewicz I. Ermüdungsfestigkeit von Stahlbeton- und Spannbetonbauteilen mit Erläuterungen zu den Nachweisen gemäß CEB-FIP Model Code 1990. Deutscher Ausschuss für Stahlbeton, Heft 439. Berlin: Beuth Verlag GmbH; 1994.
4. Bennett EW, Muir SE, St J. Some fatigue tests of high-strength concrete in axial compression. Mag Concr Res. 1967;19(59):113–7.
5. Hegger J, Roggendorf T, Goralski C, Roeser W. Ermüdungsverhalten von Beton unter zyklischer Beanspruchung aus dem Betrieb von Windkraftanlagen. 2014. Abschlussbericht des Instituts für Massivbau (IMB) der RWTH Aachen und H + P Ingenieure GmbH & Co. KG. Bauforschung T3305. Fraunhofer IRB Verlag.
6. Sparks PR, Menzies JB. The effect of rate of loading upon the static and fatigue strengths of plain concrete in compression. Mag Concr Res. 1973;25(83):73–80.
7. Göhlmann J. Zur Schädigungsberechnung von Betonkonstruktionen für Windenergieanlagen unter mehrstufiger und mehraxialer Ermüdungsbeanspruchung. Dissertation. Leibniz Universität Hannover. 2009.
8. Marx S, Grünberg J, Hansen M, Schneider S. Sachstandsbericht – Grenzzustände der Ermüdung von dynamisch hoch beanspruchten Tragwerken aus Beton. Deutscher Ausschuss für Stahlbeton. Heft 618. Berlin: Ernst & Sohn; 2017.
9. Willers K, Gerlach L, Herrmann N, Dehn F. Ermüdungscharakteristika eines hochfesten Betons bei sehr hohen Lastwechselzahlen. Beton Stahlbetonbau. 2020;115:848–57. https://doi.org/10.1002/best.202000043
10. Hohberg R. Zum Ermüdungsverhalten von Beton. Dissertation, Fakultät VI Bauingenieurwesen und Angewandte Geowissenschaften der Technischen Universität Berlin. 2004 https://doi.org/10.14279/depositonce-815
11. Holmen JO. Fatigue of concrete by constant and variable amplitude loading. 1979. Division of Concrete Structures, The Norwegian Institute of Technology, The University of Trondheim.
12. Oneschkow N, von der Haar C, Hümme J, Otto C, Lohaus L, Marx S. Ermüdung von druckschwellbeanspruchtem Beton – Materialverhalten, Modellbildung, Bemessung. In: Bergmeister K, Fingerloos F, Wörner J-D, editors. Betonkalender 2018. Reston, VA: American Society of Civil Engineers (ASCE); 2018. p. 643–756. https://doi.org/10.1002/9783433607534.ch12
13. Mu B, Subramaniam KV, Shah SP. Failure mechanism of concrete under fatigue compressive load. J Mater Civ Eng. 2004;16(6):566–72. https://doi.org/10.1061/(ASCE)0899-1561(2004)16:6(566)
14. Verbundvorhaben: WinConFat – Materialermüdung von On- und Offshore Windenergieanlagen aus Stahlbeton und Spannbeton unter hochzyklischer Beanspruchung; Teilvorhaben: Beton unter hohen Lastspielzahlen gefördert durch das Bundesministerium für Wirtschaft und Energie (FKZ: 0324016E).
15. Willers K, Gerlach L, Herrmann N, Dehn F. Untersuchungen zum Ermüdungswiderstand von Beton im Bereich sehr hoher Lastwechselzahlen. Deutscher Ausschuss für Stahlbeton, Heft 647. https://doi.org/10.25716/thm-287
16. Murdock J. A critical review of research on fatigue of plain concrete. University of Illinois Bulletin. Volume 62, Number 62, Illinois, February 1965. 1965.
17. Awad ME, Hilsdorf HK. Strength and deformation characteristics of plain concrete subjected to high repeated and sustained loads. 1971. Civil Engineering Studies, SRS No. 372, University of Illinois.
18. Weigler H, Freitag W. Dauerschwell- und Betriebsfestigkeit von Konstruktions-Leichtbeton. Deutscher Ausschuss für Stahlbeton, Heft 247. Berlin: Ernst & Sohn; 1975.
19. Klausen D. Festigkeit und Schädigung von Beton bei häufig wiederholter Beanspruchung, Dissertation. Fachbereich Konstruktiver Ingenieurbau der Technischen Hochschule Darmstadt. 1978.
20. Petkovic G, Rosseland S, Stemland H. High-strength concrete. Fatigue of High-Strength Concrete. 1992 SINTEF Structural Engineering. August 1992.
21. Nygard K, Petkovic G, Rosseland S, Stemland H. High-strength concrete. The Influence of Moisture Conditions on the Fatigue Strength of Concrete. 1992 SINTEF Structural Engineering. Report 3.1. August 1992.
22. Do M-T, Chaallal O, Aitcin P-C. Fatigue behavior of high-performance concrete. J Mater Civ Eng. 1993;5(1):96–111.
23. Kim J, Kim Y. Experimental study of the fatigue behavior of high strength concrete. Cem Concr Res. 1996;26(10):1151–523.
24. Gao L, Hsu C-TT. Fatigue of concrete under uniaxial compression cyclic loading. ACI Mater J. 1998;95(5):575–81.
25. Schwabach E. Verformungs- und Degradationsverhalten von niederzyklisch uniaxial druckbeanspruchtem Beton. Dissertation. Bauhaus-Universität Weimar, Weimar. Institut für Konstruktiven Ingenieurbau (IKI). 2005.
26. Ibuk H. Ermüdungsverhalten von Beton unter Druckschwellbelastung. Dissertation. Ruhr-Universität Bochum. 2008.
27. Breitenbücher R, Ibuk H, Osterminski K. Veränderung der Steifigkeit und des Dehnungsverhaltens von Normalbeton bei zyklischer Druckschwellbeanspruchung mit Ruhephasen. Beton Stahlbetonbau. 2007;102(2):80–7. https://doi.org/10.1002/best.200600524

28. Saucedo L, Yu RC, Medeiros A, Zhang X, Ruiz G. A probabilistic fatigue model based on the initial distribution to consider frequency effect in plain and fiber reinforced concrete. Int J Fatigue. 2013;48:308–18.
29. Thiele M. Experimentelle Untersuchung und Analyse der Schädigungsevolution in Beton unter hochzyklischen Ermüdungsbeanspruchungen. Dissertation. Fakultät VI-Planen. Bauen Umwelt der Technischen Universität Berlin 2015 https://doi.org/10.14279/depositonce-4886
30. Von der Haar C, Hümme J, Marx S, Lohaus L. Untersuchungen zum Ermüdungsverhalten eines höher-festeren Normalbetons. Beton Stahlbetonbau. 2015;110(10):699–709. https://doi.org/10.1002/best.201500034
31. Elsmeier K. Influence of temperature on the fatigue behaviour of concrete. Conference Paper. fib Symposium, Copenhagen. 2015.
32. Elsmeier K. Einfluss der Probekörpererwärmung auf den Ermüdungswiderstand von hochfestem Vergussbeton. Dissertation. Leibniz Universität Hannover, Hannover. ifB, Institut für Baustoffe. 2018.
33. Hümme J. Ermüdungsverhalten von hochfestem Beton unter Wasser. Dissertation. Gottfried Wilhelm-Leibniz-Universität Hannover. Institut für Baustoffe. 2018 https://doi.org/10.15488/3563
34. Schneider S, Hümme J, Marx S, Lohaus L. Untersuchungen zum Einfluss der Probenkörpergröße auf den Ermüdungswiderstand von hochfestem Beton. Beton Stahlbetonbau. 2018; 113(1):58–67. https://doi.org/10.1002/best.201700051
35. Tomann C, Oneschkow N. Influence of moisture content in the microstructure on the fatigue deterioration of high-strength concrete. Struct Concr. 2019;20(4):1204–11. https://doi.org/10.1002/suco.201900023
36. Tomann C. Wasserinduzierte Ermüdungsschädigung von Beton. Dissertation. Gottfried Wilhelm Leibniz Universität Hannover. Fakultät für Bauingenieurwesen und Geodäsie. 2021 https://doi.org/10.15488/11314
37. Deutscher M, Markert M, Scheerer S. Influence of temperature on the compressive strength of high performance and ultra-high performance concretes. Struct Concr. 2021;23(4):1–10. https://doi.org/10.1002/suco.202100153
38. Kachkouch FZ, Noberto CC, Babadopulos LF d AL, Melo ARS, Machado AML, Sebaibi N, Boukhelf F, Mendili E Y. Fatigue behavior of concrete: A literature review on the main relevant parameters. Constr Build Mater. 2022;338:127510. https://doi.org/10.1016/j.conbuildmat.2022.127510
39. Tepfers R, Fridén C, Georgsson L. A study of the applicability to the fatigue of concrete of the Palmgren-Miner partial damage hypothesis. Mag Concr Res. 1977; 29(100):123–30.
40. Chen Y, Ni J, Ping Z, Azzam R, Zhou Y, Shao W. Experimental research on the behaviour of high frequency fatigue in concrete. Eng Fail Anal. 2011;18(7):1848–57. https://doi.org/10.1016/j.engfailanal.2011.06.012
41. Karr U, Schuller R, Fitzka M, Denk A, Strauss A, Mayer H. Very high cycle fatigue testing of concrete using ultrasonic cycling. Mater Test. 2017;59:438–44. https://doi.org/10.3139/120.111021
42. Fitzka M, Karr U, Granzner M, Melichar T, Rödhammer M, Strauss A, Mayer H. Ultrasonic fatigue testing of concrete. Ultrasonics. 2021;116:106521. https://doi.org/10.1016/j.ultras.2021.106521
43. Erismann T. Prüfmaschinen und Prüfanlagen: Hilfsmittel der zerstörenden Materialprüfung. Berlin, Heidelberg: Springer-Verlag; 1992.
44. DIN EN 12390-13:2021-09: Testing hardened concrete – Part 13: Determination of secant modulus of elasticity in compression; German version EN 12390-13:2021.
45. DIN EN 12390-3:2019-10: Testing hardened concrete – Part 3: Compressive strength of test specimens; German version EN 12390-3:2019. Beuth-Verlag, Berlin.
46. DIN EN 12390-1:2021-09: Testing hardened concrete – Part 1: Shape, dimensions and other requirements for specimens and moulds; German version EN 12390-1:2021.
47. Lohaus L, Oneschkow N, Wefer M. Design model for the fatigue behaviour of normal-strength, high-strength and ultra-high-strength concrete. Struct Concr. 2012;13(3):182–92. https://doi.org/10.1002/suco.201100054
48. Wefer M. Materialverhalten und Bemessungswerte von ultrahochfestem Beton unter einaxialer Ermüdungs beanspruchung. Dissertation, Leibniz Universität Hannover. 2010.
49. Oneschkow N. Analyse des Ermüdungsverhaltens von Beton anhand der Dehnungsentwicklung. Dissertation, Leibniz Universität Hannover. 2014 https://doi.org/10.15488/357
50. Grünberg J, Hansen M, Göhlmann J. Bemessungsmodell für die Ermüdungsbeanspruchung bei schwingungsanfälligen turmartigen Bauwerken aus Stahlbeton und Spannbeton. 2008. Forschungsbericht Nr. 0514 des Instituts für Massivbau der Universität Hannover, Abschlussbericht DIBt-Projekt DIBt – ZP 52-5-3.85-1103/04.
51. von der Haar C. Ein mechanisch basiertes Dehnungsmodell für ermüdungsbeanspruchten Beton. Dissertation. Hannover: Leibniz Universität Hannover; 2016. https://doi.org/10.15488/8691
52. Teichen K-T. Über die innere Dämpfung von Beton. Dissertation, Universität Stuttgart. 1968.
53. von der Haar C, Wedel F, Marx S. Numerical and experimental investigations of the warming of fatigue-loaded concrete. In: Beushausen H, editor. Proceedings of fib Symposium, 21.–23.11.2016. Performance-based approaches for concrete structures. Lausanne: Cape Town; 2016.
54. Whaley CP, Neville AM. Non-elastic deformation of concrete under cyclic compression. Mag Concr Res. 1973;25(84): 145–54.
55. Elsmeier K, Lohaus L. Temperature development of concrete due to fatigue loading. In: Bastien J, Rouleau N, Fiset M, Thomassin M, editors. Proceedings, 21.–23.07.2014. The 10th fib international PhD symposium in civil engineering in Québec. Lausanne: Laval. p. 137–42.
56. von der Haar C, Marx S. Strain development of plain high strength concrete under fatigue loading. In: Fehling E, Middendorf B, Thiemicke J, editors. Proceedings of HiPerMat 2016, 4th International Symposium on Ultra-High Performance Concrete and High Performance Construction Materials, 9.–11.03.2016. Kassel: Schriftenreihe Baustoffe und Massivbau der Universität Kassel: Heft 40; 2016.

AUTHOR BIOGRAPHIES

Kerstin Willers, Karlsruhe Institute of Technology (KIT), Institute of Concrete Structures & Building Materials, Building Materials and Concrete Construction, 76131 Karlsruhe, Germany. Email: kerstin.willers@kit.edu

Lutz Gerlach, Karlsruhe Institute of Technology (KIT), Institute of Concrete Structures & Building Materials, Building Materials and Concrete Construction, 76131 Karlsruhe, Germany. Email: lutz.gerlach@kit.edu

Frank Dehn, Karlsruhe Institute of Technology (KIT), Institute of Concrete Structures & Building Materials, Building Materials and Concrete Construction, 76131 Karlsruhe, Germany. Email: frank.dehn@kit.edu

How to cite this article: Willers K, Gerlach L, Dehn F. Concrete with a very high number of load cycles—Identification of stress levels for efficient investigation of fatigue behavior. Structural Concrete. 2026. https://doi.org/10.1002/suco.70698